Weighting functions for the neutron capture measurements performed at nTOF-CERN in 2002

G. Aerts and F. Gunsing
CEA/Saclay
DSM/DAPNIA/SPhN
F-91191 Gif-sur-Yvette, France

May 15, 2002

Abstract

For neutron capture measurements with C_6D_6 liquid scintillator gamma-ray detectors at the nTOF facility at CERN, we have calculated the response functions of the detectors by means of Monte Carlo simulations with the code MCNP. In total we simulated all 34 cases in 6 different sample-detector geometries as used in the capture measurements at CERN in 2002. From the response functions for each case we derived a weighting function, which is indispensable for the analysis of neutron capture measurements with C_6D_6 detectors. The parameters of all weighting functions are given together with their statistical uncertainties.

Introduction

In neutron capture cross section experiments one measures the gamma rays following the capture of incident neutrons on a sample and inducing a (n,γ) reaction. The cross section shows resonances since the compound nucleus formed by neutron capture is in an excited state at several MeV above the ground state due to the available neutron binding energy. Many decay paths via intermediate levels to the ground state are possible, especially for medium and heavy mass nuclei with a large level density.

The signature of a (n,γ) reaction is the subsequent gamma cascade, consisting of one or more gamma rays. The corresponding gamma-ray spectrum and gamma-ray multiplicity spectrum vary from one resonance to another but also from one isotope to another. Only if all gamma rays from a cascade are detected, like in a detector with 100% efficiency and covering a 4π solid angle, the capture reaction yield can be determined in a straightforward way. With a gamma-ray detector covering a smaller solid angle or

having a smaller efficiency, such as the C_6D_6 detectors used at nTOF-CERN, not all gamma rays of the cascade are detected.

To overcome this situation, one usually applies the pulse height weighting technique, allowing to make the detection efficiency of a capture event independent from the decay cascade.

The nucleus at its excitation energy E_c, decays by a gamma-ray cascade to the ground state. The sum of the gamma-ray energies $E_{\gamma,i}$ of the cascade corresponds to E_c

$$E_c = \sum_{i=1}^{n} E_{\gamma_i} \tag{1}$$

and the detection efficiency ϵ_c of the cascade can be expressed as:

$$\epsilon_c = 1 - \prod_{i=1}^{n} (1 - \epsilon_{\gamma_i}) \tag{2}$$

with ϵ_{γ_i}, the detection efficiency of the gamma-ray i of the cascade.

If the detection efficiency for a single gamma ray is small, $\epsilon_{\gamma_i} \ll 1$, then the previous equation can be approximated by:

$$\epsilon_c \approx \sum_{i=1}^{n} \epsilon_{\gamma_i} \tag{3}$$

If the detection efficiency of the detector was proportional to the gamma-ray energy,

$$\epsilon_\gamma = k \times E_\gamma \tag{4}$$

then the cascade efficiency would be proportional to the excitation energy

$$\epsilon_c = \sum_{i=1}^{n} \epsilon_{\gamma_i} = k \times \sum_{i=1}^{n} E_{\gamma_i} = k \times E_c \tag{5}$$

Real life detectors do not have this proportionality, except in approximation the Moxon-Rae detectors [1]. It is therefore convenient to change the efficiency artificially by applying a weight to the detected events in order to establish the proportionality of equation 4. The efficiency ϵ_γ for a gamma ray is related to the response function of the detector by:

$$\epsilon_\gamma = \int R_\gamma(E) dE \tag{6}$$

The response function is the probability distribution of the energy deposited in the detector for an incident gamma ray. For a detector with an infinite resolution and a 100% efficiency, the response function is a delta function. Detectors with a low resolution have broad response functions which can be measured [2] or simulated. A function $W(E)$ of the deposited energy has to be found in order to satisfy the relation:

$$\epsilon_\gamma = \int W(E) R_\gamma(E) dE = k \times E_\gamma \tag{7}$$

When the response function is known for several gamma rays, a parametrization of $W(E)$ can be obtained by minimizing the χ^2 quantity

$$\chi^2 = \sum_{i=1}^{n} \left(\frac{E_{\gamma_i} - \sum_j W(E_j) R_{\gamma_i}(E_j)}{\sigma_i} \right)^2 \tag{8}$$

where the proportionality constant has been taken $k = 1$ and where the continuous response function $R_\gamma(E)$ of a single gamma ray has been discretized in bins j as $R_\gamma(E_j)$. A relative weight or "data uncertainty" σ_i can be attributed to each response function $R_{\gamma_i}(E)$ in the fitting procedure.

1. Simulated geometries for the capture measurements

At the newly constructed nTOF facility at CERN [3], a measurement programme has been undertaken to measure neutron capture and fission cross sections. This facility offers two main advantages: a high instantaneous neutron flux, allowing capture measurements of radioactive samples, and a large neutron energy range combined with good resolution.

To detect the gamma rays from the (n,γ) reaction, we use C_6D_6-based liquid scintillator detectors. This material has a very low neutron capture cross section and is in this way much less sensitive to neutrons scattered from the sample to the detector. Two types of C_6D_6 detectors have been used in the measurement campaign of 2002: an optimized commercial detector available from Bicron [4], and an in-house developed detector from FZK-Karlsruhe [5], with a carbon fibre housing optimized for an even lower neutron sensitivity.

In order to determine the weighting functions for the measurement setup, the detector response functions over a wide range of gamma-ray energies are necessary, typically from

0.1 to 10 MeV. Since nearly mono-energetic gamma-ray sources are not readily available above about 2.6 MeV, it is convenient to use simulations to calculate the response functions. We have used the Monte Carlo simulation code MCNP [6] to determine the detector response functions for each of the capture setups used at nTOF-CERN in 2002.

The simulations include all 34 samples measured in the 6 different main geometries. The geometry description includes the sample, the sample holder, the sample changer beam pipes and the detectors in much detail. For each sample, we simulated the energy spectrum deposited in the active C_6D_6 volume for a series of 15 mono-energetic and isotropic gamma rays of energies 0.1, 0.2, 0.5, 0.7, 0.8, 1.0, 2.0, 3.0, 4.0, 5.0, 6.0, 7.0, 8.0, 9.0 and 10.0 MeV, originating uniformly throughout the sample volume. The obtained spectra were broadened afterwards with a Gaussian broadening function with a variance of $\sigma^2 = 6E$ (σ and E in keV) [7, 8] in order to take into account the broadening due to the photomultiplier. An example of such a set of responses is shown in figure 1. Especially the double escape peaks due to pair creation are distinguishable.

In the following we describe the 6 different setups and the corresponding measured samples for part of the experiments of TOF02 [9], TOF03 [10], TOF05 [11] and TOF07 [12].

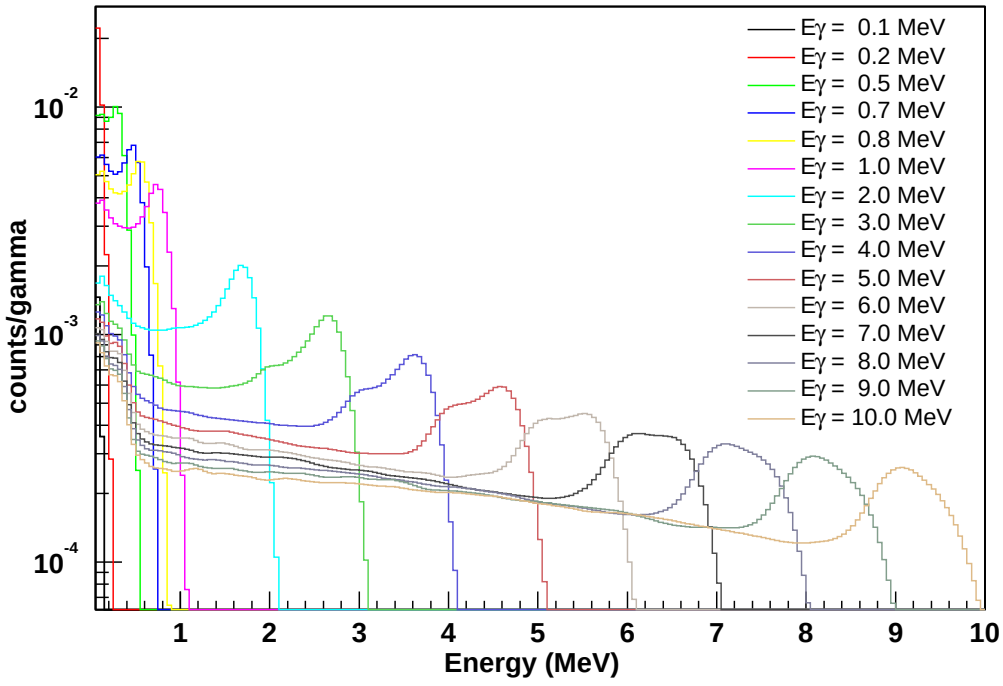

Figure 1: Detector response functions with broadening, for the case of Au (1 mm x 15 mm) used in TOF07.

1.1 Sample-detector geometry setup #1

At the start of the experiments in 2002, one Bicron and one FZK detector were in use. The distance from the center of the beam to the front of the detector is 4.1 cm and the detectors are aligned to the center of the sample. In figure 2 the Bicron detector is represented on the left and the FZK detector on the right. In table 1 the samples used in this configuration are listed. The masses and diameters are most accurate, the thickness is only approximate.

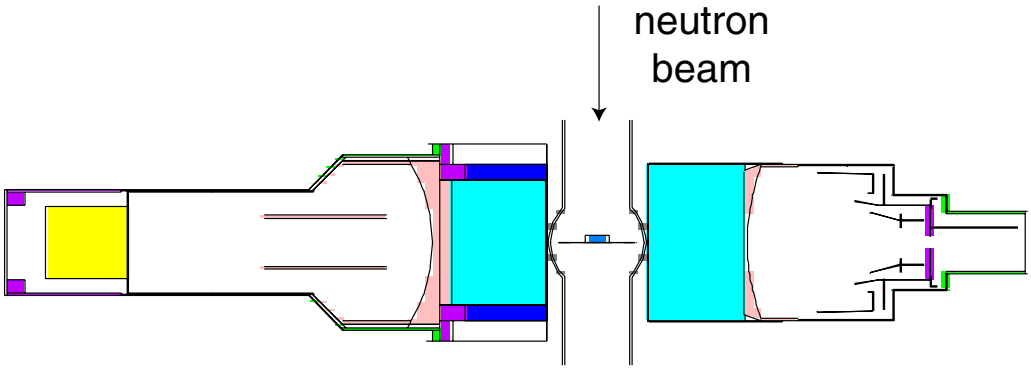

Figure 2: One of the geometries used in TOF02.

Table 1: Samples measured in setup #1.

sample number	material	thickness (mm)	diameter (mm)	mass (g)
1	Au	1.0	20.0	5.91011
2	Au	0.1	45.0	3.29
3	C	6.35	20.0	3.93345
4	Pb	1.0	20.0	3.607

1.2 Sample-detector geometry setup #2

From all other setups, two FZK detectors were used. In the configuration of figure 3 the distance from the center of the beam to the front of the detector is 4.1 cm and the detectors are aligned to the center of the sample. The corresponding samples are given in table 2.

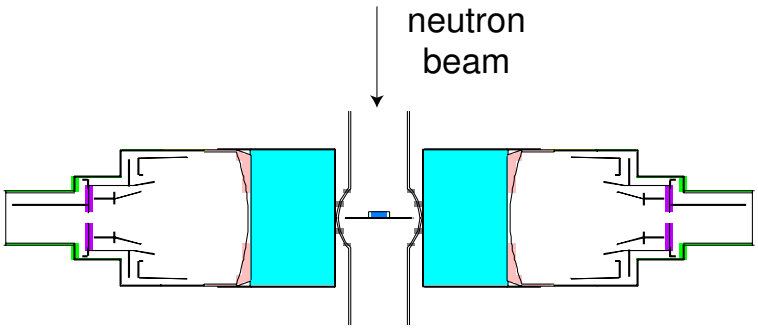

Figure 3: One of the geometries used in TOF02.

Table 2: Samples measured in setup #2.

sample number	material	thickness (mm)	diameter (mm)	mass (g)
2	Au	0.1	45.0	3.29
3	C	6.35	20.0	3.93345
5	Fe	0.5	45.0	6.17
6	Fe	2.0	45.0	25.18933

1.3 Sample-detector geometry setup #3

In order to reduce the sample-scattered photon background, the detectors were moved 7.8 cm upstream as shown in figure 4. The distance from the center of the beam to the front of the detector is 4.1 cm. The three samples measured with this configuration are given in table 3.

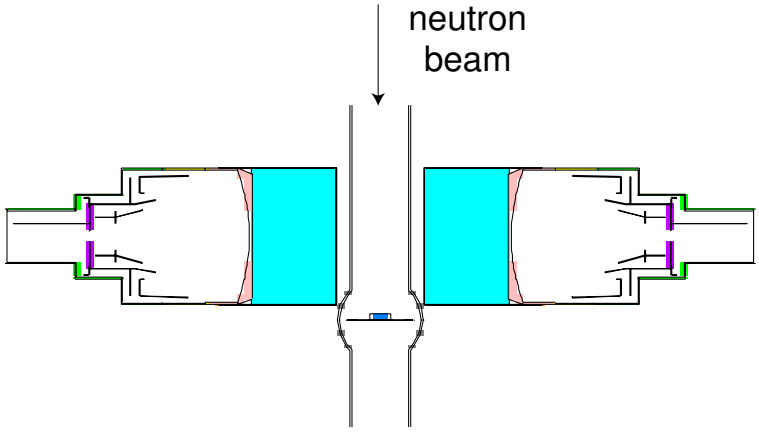

Figure 4: One of the geometries used in TOF02.

Table 3: Samples measured in setup #3.

sample number	material	thickness (mm)	diameter (mm)	mass (g)
3	C	6.35	20.0	3.93345
4	Pb	1.0	20.0	3.607
6	Fe	2.0	45.0	25.18933

1.4 Sample-detector geometry setup #4

In the setup of figure 5 the sample changer has been removed to allow the measurement of the radioactive Sm_2O_3 sample, and the related samples listed in table 4, in air. The distance from the center of the beam to the front of the detector is 2.9 cm and the detectors are shifted from the center of the sample by 9.1 cm.

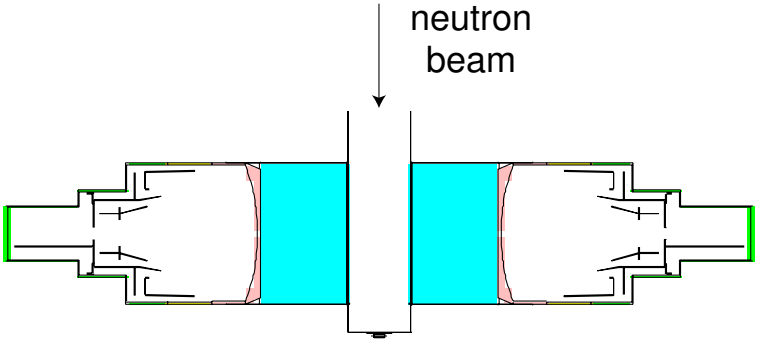

Figure 5: Geometry used for TOF03.

Table 4: Samples measured in setup #4.

sample number	material	thickness (mm)	diameter (mm)	mass (g)
7	Au	1.0	10.0	1.48556
8	Sm_2O_3	2.4	10.0	0.2064
9	C	1.5	10.0	0.23062
10	Pb	1.0	10.0	0.95745

1.5 Sample-detector geometry setup #5

In the setup in figure 6 with samples from table 5 the distance from the center of the beam is 4.0 cm and the detectors are shifted from the center of the sample by 7.8 cm.

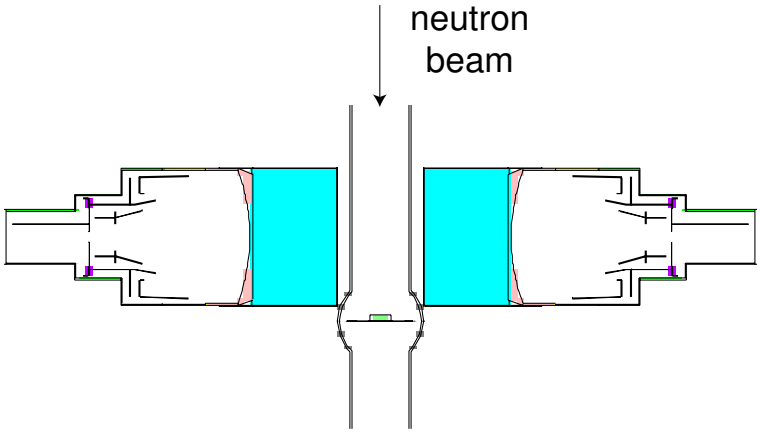

Figure 6: One of the geometries used in TOF05.

Table 5: Samples measured in setup #5.

sample number	material	thickness (mm)	diameter (mm)	mass (g)
1	Au	1.0	20.0	5.91011
3	C	6.35	20.0	3.93345
11	Fe	2.0	20.0	4.85285
12	^{209}Bi	6.08	20.0	18.90453
13	^{208}Pb	3.6	20.0	12.53146
14	Au	0.125	20.0	0.75506
15	^{207}Pb	2.21	20.05	8.00925
16	^{204}Pb	1.18	20.08	4.0389
17	^{206}Pb	2.27	20.03	8.12025

1.6 Sample-detector geometry setup #6

In this setup shown in figure 7 the distance from the center of the beam is 2.9 cm and the detectors are shifted from the center of the sample by 9.2 cm. Samples measured in this configuration are given in table 6.

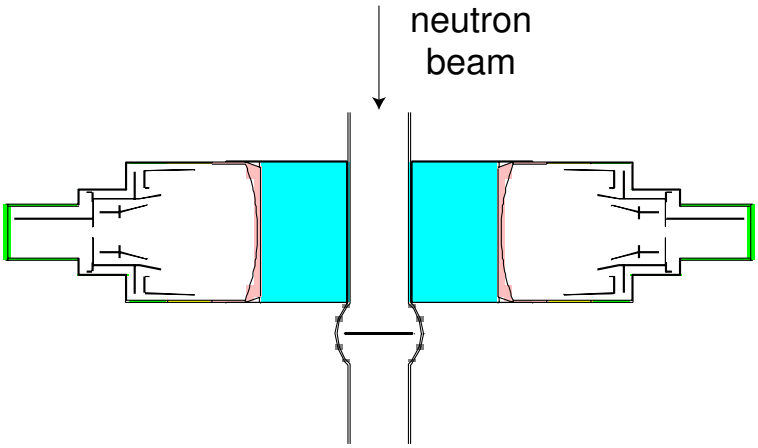

Figure 7: Geometry used in TOF05 and tin TOF07.

Table 6: Samples measured in setup #6.

sample number	material	thickness (mm)	diameter (mm)	mass (g)
16	^{204}Pb	1.18	20.08	4.0389
17	^{206}Pb	2.27	20.03	8.12025
18	Au	0.5	20.0	2.95236
19	Pb nat	1.09	15.485	2.0434
20	Au	0.53	15.04	0.8843
		0.28	15.125	0.4454
21	Th	0.5	15.125	1.0262
		0.85	15.125	1.7784

2. Weighting functions

From the simulated and subsequently broadened response functions we derived a weighting function by minimizing equation (8). We got best results with a third order polynomial for $W(E)$

$$W(E) = \sum_{k=0}^{3} a_k E^k \tag{9}$$

In the fitting procedure we used a relative weight or "data uncertainty" for each gamma response function i equal to

$$\sigma_i = E_{\gamma_i} \frac{\sqrt{\sum_j dR^2_{\gamma_i}(E_j)}}{\sum_j R_{\gamma_i}(E_j)} \tag{10}$$

From the fit are resulting the optimized parameters and the covariance matrix of the parameters. The variance of the weighting function with m parameters a_k is then given in a general form by

$$\mathrm{var}(W(E)) = \sum_{i=0}^{m} \sum_{j=0}^{m} \left(\frac{\partial W}{\partial a_i}\right) \left(\frac{\partial W}{\partial a_j}\right) \mathrm{cov}(a_i, a_j) \tag{11}$$

which becomes in the case of a polynomial

$$\mathrm{var}(W(E)) = \sum_{i=0}^{m} \sum_{j=0}^{m} E^i E^j \mathrm{cov}(a_i, a_j) \tag{12}$$

Instead of the covariance matrix it is sometimes easier to use the correlation matrix defined by

$$\rho(a_i, a_j) = \frac{\sqrt{\mathrm{var}(a_i)\mathrm{var}(a_j)}}{\mathrm{cov}(a_i, a_j)} \tag{13}$$

In the annexe we give the correlation coefficients in percent for ease of reading.

The uncertainty on the fitted function resulting from standard fitting procedures can be unrealistically small if the uncertainties on the data σ_i are small. Especially with Monte Carlo simulations it is easy to increase the number of events in order to improve the statistical counting errors. Although small uncertainties are then obtained, the goodness

of the fit is characterized by the reduced chi-square value, the chi-square divided by the number of degrees of freedom, which should be in the order of 1 for a statistically coherent fit assuming Gaussian errors. A high value of the reduced chi-square may indicate that the chosen fitting function is not well adapted to the data.

A commonly used compromise for the situation of a fit with small parameter uncertainties and a high reduced chi-square value, is to scale the data uncertainties σ_i with a factor F in order to obtain a reduced chi-square of 1. The number of degrees of freedom corresponds to the number of gamma-ray spectra n minus the number of parameters k.

$$\frac{\chi^2}{n-k} = \sum_{i=1}^{n} \left(\frac{E_{\gamma_i} - \sum_j W(E_j) R_{\gamma_i}(E_j)}{F \times \sigma_i} \right)^2 = 1 \qquad (14)$$

In table 7 we summarize the fitted parameters for the weighting functions of all 34 cases. The response function below 200 keV were not included in the fit, which corresponds to the threshold typically used in the data analysis.

Depending on the sample the weighting functions can have a very different shape for a same geometry. The attenuation and pair creation are in fact quite different for different samples. This is illustrated in figure 8 for 3 samples in the same setup.

Also the Bicron and FZK detectors have different efficiencies, mainly due to the differ-

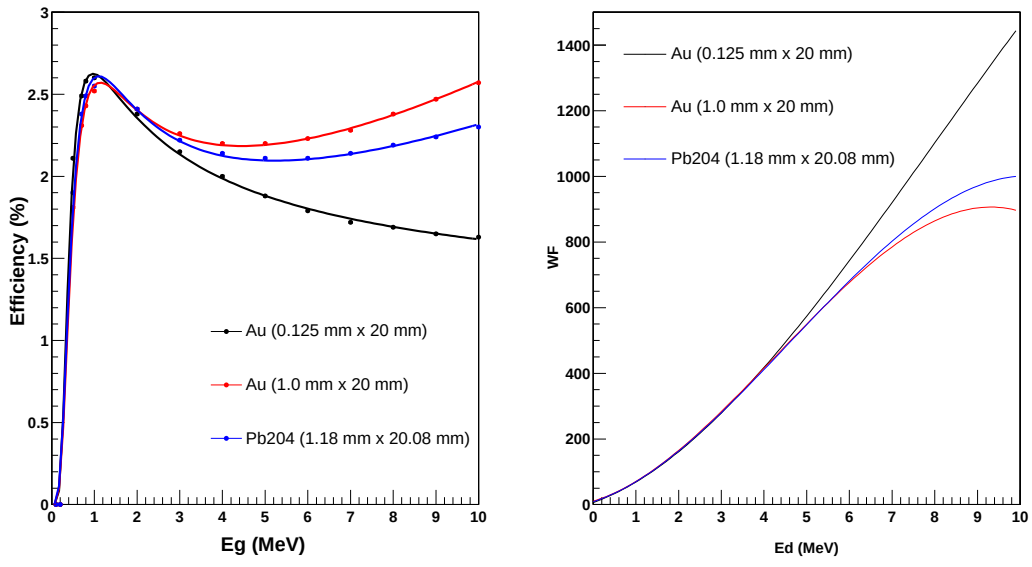

Figure 8: Detector efficiency and weighting function for the same configuration #5 but for different samples: Au (0.125 mm x 20 mm), Au (1.0 mm x 20 mm) and 204Pb (1.18 mm x 20.08 mm).

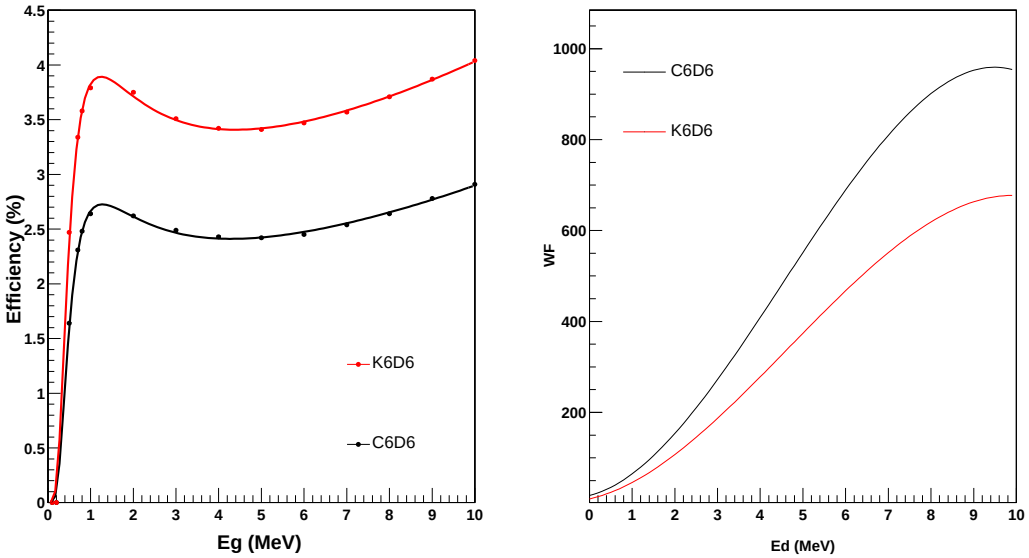

Figure 9: The detector efficiencies on the left and the related weighting function on the right for the case of Au (1.0 mm x 20 mm) in setup #1.

ent volume of C_6D_6. In figure 9 the efficiencies for both detectors and corresponding weighting functions are shown. The roughly 50% higher efficiency for the FZK detectors is directly related to the about 50% larger volume of liquid scintillator.

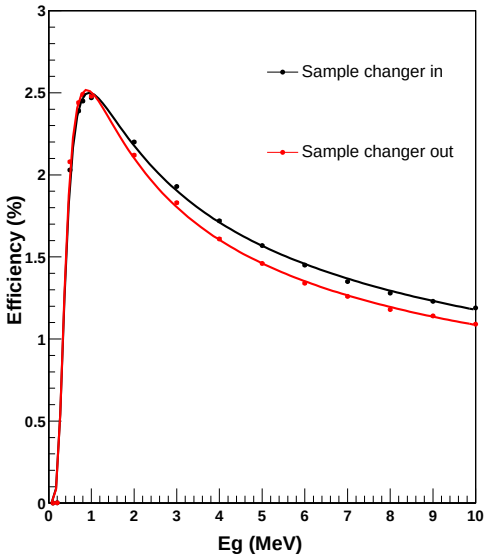

Figure 10: Detector efficiencies with and without the sample changer present in the simulation.

Table 7: The weighting functions for a single detector for the capture experiments at CERN in 2002. The parameters correspond to a third order polynomial $\sum_k a_k E^k$. Uncertainties related to these parameters are given in the annexe.

setup	sample	experiment	detector	a_0	a_1	a_2	a_3
1	1	TOF02	FZK	9.746	20.962	16.180	16.180
1	1	TOF02	Bicron	17.265	22.967	26.516	26.516
1	2	TOF02	FZK	4.726	24.648	11.306	11.306
1	2	TOF02	Bicron	7.648	33.158	17.083	17.083
1	3	TOF02	FZK	3.049	30.614	8.873	8.873
1	3	TOF02	Bicron	5.469	41.349	13.612	13.612
1	4	TOF02	FZK	7.593	22.800	14.284	14.284
1	4	TOF02	Bicron	12.980	28.172	22.492	22.492
2	2	TOF02	FZK	4.590	24.915	11.165	11.165
2	3	TOF02	FZK	2.722	31.392	8.484	8.484
2	5	TOF02	FZK	3.506	28.134	9.623	9.623
2	6	TOF02	FZK	5.027	27.667	11.485	11.485
3	3	TOF02	FZK	5.886	47.845	15.545	15.545
3	4	TOF02	FZK	8.558	43.345	20.432	20.432
3	6	TOF02	FZK	6.162	47.694	17.614	17.614
4	7	TOF03	FZK	8.980	48.042	21.993	21.993
4	8	TOF03	FZK	6.118	48.810	18.354	18.354
4	9	TOF03	FZK	6.265	51.423	18.380	18.380
4	10	TOF03	FZK	7.807	49.703	20.559	20.559
5	1	TOF05	FZK	10.684	38.929	22.632	22.632
5	3	TOF05	FZK	5.679	47.417	15.198	15.198
5	11	TOF05	FZK	6.451	46.734	17.605	17.605
5	12	TOF05	FZK	19.938	27.822	27.928	27.928
5	13	TOF05	FZK	16.948	29.975	26.897	26.897
5	14	TOF05	FZK	6.247	46.172	17.026	17.026
5	15	TOF05	FZK	13.264	34.689	24.517	24.517
5	16	TOF05	FZK	8.936	41.777	20.691	20.691
5	17	TOF05	FZK	13.680	33.778	24.948	24.948
6	16	TOF05	FZK	8.955	44.610	21.024	21.024
6	17	TOF05	FZK	13.869	35.344	25.488	25.488
6	18	TOF05	FZK	7.360	48.171	19.158	19.158
6	19	TOF07	FZK	8.038	46.692	19.860	19.860
6	20	TOF07	FZK	6.138	51.054	17.763	17.763
6	21	TOF07	FZK	9.242	44.225	21.370	21.370

Another element affecting the efficiency is the surrounding material. The increase of pair production due to material between the detector and the sample is well illustrated by the non-negligible effect of the carbon fibre tube from the sample changer. In figure 10 this effect is shown.

Conclusions

This note contains the weighting functions obtained from simulations of detector responses with MCNP for all 34 detector-sample setups used in 2002 at CERN. In parallel other groups (IFIC and INFN) have been working on weighting functions using different simulation codes. A comparison between the results of the different codes aims to validate all calculations. But it should be stressed that it is not necessary to have identical weighting functions for a correct analysis. Weighting functions with a different shape may give very similar weighted spectra. In addition, the weighted capture spectra are used relative to weighted spectra of a standard, which may minimize possible systematic uncertainties resulting from the applied weighting function.

References

[1] M. Moxon and E. Rae, *Nucl. Instr. and Meth.* 24 (1963) 445.

[2] J. N. Wilson *et al.* , *Measurements of (n,γ) neutron capture cross sections with liquid scintillator detectors* (2003), accepted for publication in Nucl. Instr. Meth. A.

[3] The nTOF collaboration, *CERN nTOF Facility: Performance Report*, CERN/INTC-O-011, INTC-2002-037, CERN-SL-2002-053 ECT (2003)

[4] http://www.bicron.com

[5] R. Plag *et al.* , *An optimized C6D6 detector for studies of resonance-dominated (n,γ) cross-sections*, Nucl. Instr. Meth. A496 (2003) 425

[6] J. F. Briesmeister, Ed., *MCNP - A General Monte Carlo N-Particle Transport Code, Version 4C*, LA-13709-M (2000), version 4C3

[7] J. L. Tain *et al.* , *J. Nucl. Sci. Tech.*, Suppl. 2 (2002) 689

[8] The nTOF Collaboration, *New Experimental Validation of the Pulse Height Weighting Technique for Capture Cross Section Measurements*, submitted for publication in Nucl. Instr. Meth. A.

[9] The nTOF Collaboration, *Determination of the neutron fluence, the beam characteristics and the backgrounds at the CERN-PS TOF Facility*, CERN/INTC 2000-016, INTC/P123, TOF02

[10] The nTOF Collaboration, *The importance of ^{22}Ne(α,n)^{25}Mg as s-process neutron source and the s-process thermometer ^{151}Sm*, CERN/INTC 2000-017, INTC/P124, TOF03

[11] The nTOF Collaboration, *Neutron Cross Sections for the Pb Isotopes: Implications for ADS and Nucleosynthesis*, CERN/INTC 2001-020, INTC/P142, TOF05

[12] The nTOF Collaboration, *Measurement of the neutron capture cross sections of ^{232}Th, ^{231}Pa, ^{234}U and ^{236}U*, CERN/INTC 2002-013, INTC/P154, TOF07

Annexe

setup 1 - sample 1 - TOF02 - FZK

#	parameter	uncertainty	%	covariance matrix			
0	9.74617E+00	1.08207E+00	11.1	100	-92	83	-76
1	2.09622E+01	2.13514E+00	10.2	-92	100	-97	92
2	1.61801E+01	7.76134E-01	4.8	83	-97	100	-99
3	-1.16030E+00	6.92455E-02	6.0	-76	92	-99	100

setup 1 - sample 1 - TOF02 - Bicron

#	parameter	uncertainty	%	covariance matrix			
0	1.72645E+01	1.58898E+00	9.2	100	-92	83	-76
1	2.29668E+01	3.16940E+00	13.8	-92	100	-97	92
2	2.65160E+01	1.16825E+00	4.4	83	-97	100	-99
3	-1.94696E+00	1.05467E-01	5.4	-76	92	-99	100

setup 1 - sample 2 - TOF02 - FZK

#	parameter	uncertainty	%	covariance matrix			
0	4.72575E+00	5.07834E-01	10.7	100	-91	83	-77
1	2.46477E+01	1.01697E+00	4.1	-91	100	-97	93
2	1.13057E+01	3.69474E-01	3.3	83	-97	100	-99
3	-4.75600E-01	3.27970E-02	6.9	-77	93	-99	100

setup 1 - sample 2 - TOF02 - Bicron

#	parameter	uncertainty	%	covariance matrix			
0	7.64800E+00	1.23533E+00	16.2	100	-92	84	-77
1	3.31579E+01	2.51412E+00	7.6	-92	100	-97	93
2	1.70826E+01	9.28139E-01	5.4	84	-97	100	-99
3	-8.21980E-01	8.34825E-02	10.2	-77	93	-99	100

setup 1 - sample 3 - TOF02 - FZK

#	parameter	uncertainty	%	covariance matrix			
0	3.04937E+00	6.96926E-01	22.9	100	-91	83	-77
1	3.06142E+01	1.39925E+00	4.6	-91	100	-97	93
2	8.87330E+00	5.07092E-01	5.7	83	-97	100	-99
3	-8.61775E-02	4.48314E-02	52.0	-77	93	-99	100

setup 1 - sample 3 - TOF02 - Bicron

#	parameter	uncertainty	%	covariance matrix			
0	5.46914E+00	1.06007E+00	19.4	100	-91	83	-77
1	4.13489E+01	2.15700E+00	5.2	-91	100	-97	93
2	1.36121E+01	7.93431E-01	5.8	83	-97	100	-99
3	-2.74886E-01	7.10025E-02	25.8	-77	93	-99	100

setup 1 - sample 4 - TOF02 - FZK

#	parameter	uncertainty	%	covariance matrix			
0	7.59329E+00	8.80651E-01	11.6	100	-92	83	-77
1	2.27995E+01	1.74946E+00	7.7	-92	100	-97	93
2	1.42836E+01	6.36958E-01	4.5	83	-97	100	-99
3	-9.36236E-01	5.67350E-02	6.1	-77	93	-99	100

setup 1 - sample 4 - TOF02 - Bicron

#	parameter	uncertainty	%	covariance matrix			
0	1.29802E+01	1.31901E+00	10.2	100	-92	84	-77
1	2.81716E+01	2.65038E+00	9.4	-92	100	-97	93
2	2.24919E+01	9.78384E-01	4.3	84	-97	100	-99
3	-1.51406E+00	8.81953E-02	5.8	-77	93	-99	100

setup 2 - sample 2 - TOF02 - FZK

#	parameter	uncertainty	%	covariance matrix			
0	4.59017E+00	6.76201E-01	7.4	100	-91	83	-77
1	2.49151E+01	1.35129E+00	2.7	-91	100	-97	93
2	1.11650E+01	4.90686E-01	2.2	83	-97	100	-99
3	-4.60924E-01	4.35532E-02	4.7	-77	93	-99	100

setup 2 - sample 3 - TOF02 - FZK

#	parameter	uncertainty	%	covariance matrix			
0	2.72158E+00	7.54588E-01	13.9	100	-91	83	-77
1	3.13923E+01	1.51276E+00	2.4	-91	100	-97	93
2	8.48423E+00	5.48163E-01	3.2	83	-97	100	-99
3	-4.14395E-02	4.84576E-02	58.5	-77	93	-99	100

setup 2 - sample 5 - TOF02 - FZK

#	parameter	uncertainty	%	covariance matrix			
0	3.50582E+00	7.41657E-01	10.6	100	-91	83	-77
1	2.81339E+01	1.48980E+00	2.6	-91	100	-97	93
2	9.62345E+00	5.41828E-01	2.8	83	-97	100	-99
3	-2.68481E-01	4.80934E-02	9.0	-77	93	-99	100

setup 2 - sample 6 - TOF02 - FZK

#	parameter	uncertainty	%	covariance matrix			
0	5.02689E+00	7.84185E-01	7.8	100	-92	83	-77
1	2.76672E+01	1.57997E+00	2.9	-92	100	-97	93
2	1.14848E+01	5.77175E-01	2.5	83	-97	100	-99
3	-6.05752E-01	5.13630E-02	4.2	-77	93	-99	100

setup 3 - sample 3 - TOF02 - FZK

#	parameter	uncertainty	%	covariance matrix			
0	5.88642E+00	1.40687E+00	12.0	100	-91	83	-76
1	4.78450E+01	2.75388E+00	2.9	-91	100	-97	92
2	1.55451E+01	9.68546E-01	3.1	83	-97	100	-99
3	-3.74189E-01	8.34675E-02	11.2	-76	92	-99	100

setup 3 - sample 4 - TOF02 - FZK

#	parameter	uncertainty	%	covariance matrix			
0	8.55799E+00	1.72777E+00	10.1	100	-91	83	-76
1	4.33454E+01	3.40164E+00	3.9	-91	100	-97	93
2	2.04315E+01	1.20444E+00	2.9	83	-97	100	-99
3	-1.44761E+00	1.04429E-01	3.6	-76	93	-99	100

setup 3 - sample 6 - TOF02 - FZK

#	parameter	uncertainty	%	covariance matrix			
0	6.16232E+00	1.15115E+00	9.3	100	-91	83	-76
1	4.76941E+01	2.29387E+00	2.4	-91	100	-97	93
2	1.76136E+01	8.14039E-01	2.3	83	-97	100	-99
3	-9.66871E-01	7.05523E-02	3.6	-76	93	-99	100

setup 4 - sample 7 - TOF03 - FZK

#	parameter	uncertainty	%	covariance matrix			
0	8.97983E+00	2.26998E+00	12.6	100	-91	83	-76
1	4.80417E+01	4.44054E+00	4.6	-91	100	-97	92
2	2.19929E+01	1.55664E+00	3.5	83	-97	100	-99
3	-1.60312E+00	1.34352E-01	4.2	-76	92	-99	100

setup 4 - sample 8 - TOF03 - FZK

#	parameter	uncertainty	%	covariance matrix			
0	6.11827E+00	1.89918E+00	15.5	100	-91	82	-76
1	4.88096E+01	3.71331E+00	3.8	-91	100	-97	92
2	1.83536E+01	1.29708E+00	3.5	82	-97	100	-99
3	-5.10947E-01	1.11125E-01	10.9	-76	92	-99	100

setup 4 - sample 9 - TOF03 - FZK

#	parameter	uncertainty	%	covariance matrix			
0	6.26481E+00	1.95559E+00	15.6	100	-91	82	-76
1	5.14231E+01	3.80871E+00	3.7	-91	100	-97	92
2	1.83797E+01	1.32426E+00	3.6	82	-97	100	-99
3	-4.25592E-01	1.13102E-01	13.3	-76	92	-99	100

setup 4 - sample 10 - TOF03 - FZK

#	parameter	uncertainty	%	covariance matrix			
0	7.80684E+00	2.12697E+00	13.6	100	-91	83	-76
1	4.97033E+01	4.15758E+00	4.2	-91	100	-97	93
2	2.05588E+01	1.45829E+00	3.5	83	-97	100	-99
3	-1.33361E+00	1.25629E-01	4.7	-76	93	-99	100

setup 5 - sample 1 - TOF05 - FZK

#	parameter	uncertainty	%	covariance matrix			
0	1.06843E+01	1.83817E+00	8.6	100	-91	83	-76
1	3.89286E+01	3.60941E+00	4.6	-91	100	-97	92
2	2.26322E+01	1.27339E+00	2.8	83	-97	100	-99
3	-1.77003E+00	1.10395E-01	3.1	-76	92	-99	100

setup 5 - sample 3 - TOF05 - FZK

#	parameter	uncertainty	%	covariance matrix			
0	5.67882E+00	1.30514E+00	11.5	100	-91	83	-76
1	4.74173E+01	2.55300E+00	2.7	-91	100	-97	92
2	1.51977E+01	8.97555E-01	3.0	83	-97	100	-99
3	-3.59180E-01	7.73322E-02	10.8	-76	92	-99	100

setup 5 - sample 11 - TOF05 - FZK

#	parameter	uncertainty	%	covariance matrix			
0	6.45075E+00	1.39495E+00	10.8	100	-91	83	-76
1	4.67341E+01	2.76380E+00	3.0	-91	100	-97	93
2	1.76053E+01	9.78089E-01	2.8	83	-97	100	-99
3	-8.93509E-01	8.46312E-02	4.7	-76	93	-99	100

setup 5 - sample 12 - TOF05 - FZK

#	parameter	uncertainty	%	covariance matrix			
0	1.99376E+01	1.92074E+00	4.8	100	-92	82	-75
1	2.78221E+01	3.63016E+00	6.5	-92	100	-97	92
2	2.79279E+01	1.26097E+00	2.3	82	-97	100	-99
3	-2.02565E+00	1.09063E-01	2.7	-75	92	-99	100

setup 5 - sample 13 - TOF05 - FZK

#	parameter	uncertainty	%	covariance matrix			
0	1.69484E+01	1.89349E+00	5.6	100	-92	82	-75
1	2.99746E+01	3.63870E+00	6.1	-92	100	-97	92
2	2.68971E+01	1.27138E+00	2.4	82	-97	100	-99
3	-2.02630E+00	1.10023E-01	2.7	-75	92	-99	100

setup 5 - sample 14 - TOF05 - FZK

#	parameter	uncertainty	%	covariance matrix			
0	6.24735E+00	1.33622E+00	10.7	100	-91	83	-76
1	4.61720E+01	2.62131E+00	2.8	-91	100	-97	93
2	1.70259E+01	9.24663E-01	2.7	83	-97	100	-99
3	-7.09434E-01	7.98700E-02	5.6	-76	93	-99	100

setup 5 - sample 15 - TOF05 - FZK

#	parameter	uncertainty	%	covariance matrix			
0	1.32637E+01	1.62944E+00	6.1	100	-91	83	-76
1	3.46888E+01	3.16731E+00	4.6	-91	100	-97	92
2	2.45168E+01	1.11302E+00	2.3	83	-97	100	-99
3	-1.86255E+00	9.64221E-02	2.6	-76	92	-99	100

setup 5 - sample 16 - TOF05 - FZK

#	parameter	uncertainty	%	covariance matrix			
0	8.93589E+00	1.66822E+00	9.3	100	-91	83	-76
1	4.17768E+01	3.27860E+00	3.9	-91	100	-97	93
2	2.06909E+01	1.15933E+00	2.8	83	-97	100	-99
3	-1.49539E+00	1.00482E-01	3.4	-76	93	-99	100

setup 5 - sample 17 - TOF05 - FZK

#	parameter	uncertainty	%	covariance matrix			
0	1.36796E+01	1.75026E+00	6.4	100	-91	83	-76
1	3.37783E+01	3.40255E+00	5.0	-91	100	-97	92
2	2.49477E+01	1.19593E+00	2.4	83	-97	100	-99
3	-1.90605E+00	1.03639E-01	2.7	-76	92	-99	100

setup 6 - sample 16 - TOF05 - FZK

#	parameter	uncertainty	%	covariance matrix			
0	8.95505E+00	1.42538E+00	8.0	100	-91	83	-76
1	4.46096E+01	2.79418E+00	3.1	-91	100	-97	92
2	2.10239E+01	9.81702E-01	2.3	83	-97	100	-99
3	-1.50431E+00	8.45815E-02	2.8	-76	92	-99	100

setup 6 - sample 17 - TOF05 - FZK

#	parameter	uncertainty	%	covariance matrix			
0	1.38685E+01	1.60882E+00	5.8	100	-91	82	-75
1	3.53441E+01	3.12401E+00	4.4	-91	100	-97	92
2	2.54875E+01	1.09087E+00	2.1	82	-97	100	-99
3	-1.93444E+00	9.39385E-02	2.4	-75	92	-99	100

setup 6 - sample 18 - TOF05 - FZK

#	parameter	uncertainty	%	covariance matrix			
0	7.35995E+00	1.35273E+00	9.2	100	-91	83	-76
1	4.81713E+01	2.66184E+00	2.8	-91	100	-97	93
2	1.91583E+01	9.38107E-01	2.4	83	-97	100	-99
3	-1.32025E+00	8.09466E-02	3.1	-76	93	-99	100

setup 6 - sample 19 - TOF07 - FZK

#	parameter	uncertainty	%	covariance matrix			
0	8.03751E+00	1.50247E+00	9.3	100	-91	83	-76
1	4.66920E+01	2.94217E+00	3.2	-91	100	-97	93
2	1.98600E+01	1.03352E+00	2.6	83	-97	100	-99
3	-1.32495E+00	8.89844E-02	3.4	-76	93	-99	100

setup 6 - sample 20 - TOF07 - FZK

#	parameter	uncertainty	%	covariance matrix			
0	6.13827E+00	1.39320E+00	11.3	100	-91	83	-76
1	5.10540E+01	2.73820E+00	2.7	-91	100	-97	93
2	1.77626E+01	9.63944E-01	2.7	83	-97	100	-99
3	-1.09262E+00	8.30571E-02	3.8	-76	93	-99	100

setup 6 - sample 21 - TOF07 - FZK

#	parameter	uncertainty	%	covariance matrix			
0	9.24227E+00	1.49697E+00	8.1	100	-91	83	-76
1	4.42254E+01	2.92413E+00	3.3	-91	100	-97	92
2	2.13701E+01	1.02439E+00	2.4	83	-97	100	-99
3	-1.51219E+00	8.81241E-02	2.9	-76	92	-99	100